Pathogenesis in Aspergillus Ear Rot of Maize: Light Microscopy of Fungal Spread from Wounds

M. G. Smart, D. T. Wicklow, and R. W. Caldwell

First and second authors: Fermentation Biochemistry Research Unit and Mycotoxin Research Unit, USDA-ARS, Northern Regional Research Center, 1815 North University Street, Peoria, IL 61604. Third author: Department of Plant Pathology, Russell Laboratories, 1630 Linden Drive, University of Wisconsin, Madison, WI 53706.

The mention of firm names or trade products does not imply endorsement or recommendation by the U.S. Department of Agriculture over other firms or similar products not mentioned.

We wish to thank Mr. C. E. Needham for drawing the diagram (Fig. 1). We thank Dr. C. G. Crawford (ARS, Peoria, IL) who coached us ably in the three-dimensional reconstructions. Ms. Lola Elam worked long and searched diligently for aflatoxin in the preliminary experiment. One of us (M. G. S.) again thanks the donor for the kidney.

Accepted for publication 21 February 1990.

ABSTRACT

Smart, M. G., Wicklow, D. T., and Caldwell, R. W. 1990. Pathogenesis in aspergillus ear rot of maize: Light microscopy of fungal spread from wounds. Phytopathology 80:1287-1294.

We describe the histology of fungal development in maize ears wound inoculated with *Aspergillus flavus*. Plants were inoculated 21 days after style emergence; wounded grains and adjacent spikelets (with their rachis segments) were harvested at intervals up to 28 days later. Tissues were processed for plastic embedding and 1.5-μm thick sections were examined by bright field microscopy. The fungus spread from the wound sometime after 14 days postinoculation, and at 28 days postinoculation it could be found in small amounts throughout all rachis tissues except the pith and lignified fibers. The fungus entered the rachillae of adjacent spikelets from the rachis and also from the bracts at their insertion point. The fungus grew through the aerenchyma in the rachilla to the floral axis and innermost layers of the pericarp (the endocarp). Hyphae did not penetrate to the endocarp from the exterior of the pericarp. The hyphae were always intercellular in the rachis, rachilla, and pericarp. They were both inter- and intracellular in the floral axis and internal to the testa (i.e., inside the seed proper). From the endocarp, entry into the seed was not across the black layer; random tears in the testa over the embryo were the probable immediate pathway. Hyphae were vacuolate everywhere except in the seed. Host cells died (and even collapsed) ahead of the fungus, but no other structural alterations were seen.

Additional keywords: aflatoxin, histopathology, mycotoxin, *Zea mays*.

Ear rot of maize caused by *Aspergillus flavus* Link:Fr. is an important disease, despite its intermittent and often sporadic occurrence, because of the accumulation of aflatoxins (2). The disease has been known at least from the beginning of this century (24; and references therein), but its investigation usually has involved indirect plating methods (5,6,13,19,23,24,28,29). Marsh and Payne (15) have published a scanning electron microscopy study of disease progress after style (silk) inoculation. The styles at the honey-brown stage of senescence allow the growth of hyphae to the grain attachment site. The authors could find no internal invasion of the seed proper (that is, inside the testa, otherwise called the seed coat) but could find hyphae in the proximal rachilla (pedicel, tip cap). They proposed that *A. flavus*, behaving much like other ear-rotting pathogens (4,10,14), invaded the proximal rachilla after having grown over the pericarp. Marsh and Payne (15) did not suggest how *A. flavus* might penetrate the rachilla and neither does the older literature that deals with other ear-rotting fungi (cited above), except that *Diplodia zeae* (Schwein.) Lév entered "the pedicel [the rachilla] near the bases of the glumes or . . . entered from the cob" (4). There is little consideration given in the literature to the possibility that *A. flavus* might spread from spikelet to spikelet through the rachis (cob). In cotton, however, the fungus apparently can invade bolls via the vascular system (9) after inoculation of nectaries and other natural openings (8,9).

As described in a previous paper (22), we have observed that *A. flavus* randomly invades maize seeds. The observed pattern was consistent with the testa forming a barrier to invasion. Our data could not discriminate between the two possible modes of fungal spread from a wound: through the rachis or over outer surfaces with entry into the ear at the rachilla or grain pericarp. In this paper, we follow the growth of *A. flavus* hyphae from a wound-inoculation site to the adjacent, unwounded spikelets by using light microscopy of sectioned tissues. We focus particularly on how the fungus arrives in the rachilla and on subsequent entry into the seed proper. In so doing, we develop a model of pathogenesis for this fungus.

There is surprisingly little information in the literature on the anatomy of maize ears. The overall morphology of the ear is well understood, as is the course of the vascular bundles (7,12,21). The anatomy of the caryopsis (grain) itself has also been studied (26,27,30–33). Unfortunately, we are left with no published details of the anatomy of the rachilla or the underlying rachis. In the paragraphs which follow, we outline the general features of maize ear anatomy using mostly our own observations, supported by the information in the literature where it exists. The new information presented here is essential to an understanding of the pathology but will be published in full elsewhere.

The center of the ear is occupied by a pith (Fig. 1). The cells are large, unlignified, and highly vacuolate, with large airspaces between them. The pith grades into an unlignified parenchyma at its outer edge. Again, these parenchyma cells have large airspaces between them, but the cell walls are thicker than those of the pith. Large vascular bundles, which traverse the rachis from base to apex, are found at regular intervals along the boundary. Their anatomy (and that of all other rachis vascular bundles) is similar to previously published micrographs of bundles in other parts of the maize plant (e.g., 3), except that the bundle-sheath cells have thicker, more heavily lignified cell walls. In the region of departure of the rachilla traces, these vascular bundles are ensheathed by an aerenchyma. These aerenchyma cells are elongated along the axis of the bundle; and histochemial tests show them to have unlignified, cuticularized walls (*unpublished observations*). The cells possess short arms which radiate to other aerenchyma cells, giving the effect of so many "ladders" in longitudinal sections. The intercellular spaces, of course, are enormous, and we have estimated them to comprise 50% of the final volume of this tissue.

The rachilla vascular bundle traces which diverge from these major bundles also are ensheathed by an aerenchyma and arise

in pairs (27). The ground tissues interposed between all of these vascular bundles become increasingly more thick walled and lignified toward the epidermis. The intercellular spaces become smaller until, just beneath the epidermis, two types of fibers occur. The first type consists of cells with lignified primary walls and thick, unlignified, mucilaginous secondary walls. Small intercellular spaces occur. The other type consists of normal, fully lignified fibers with few or no intercellular airspaces. The epidermis of the rachis is unlignified, cuticularized, and uniseriate, with very few stomata. The "outer" system of small vascular bundles (12,21) interconnect with each other and, probably, with the rachilla traces, but they do not have an aerenchyma associated with them.

The rachilla itself consists of a varible number of central vascular bundles interspersed in and surrounded by an aerenchyma. Just beneath the rachilla edidermis is a multiseriate hypodermis. These cells are fibrous, having thick, lignified walls and no airspaces. The epidermis is uniseriate, cuticularized, unlignified, and almost devoid of stomata (although stomata do occur on the abaxial surfaces of bracts). The curious anatomy of the rachilla at the insertion zones of bracts will be described below in the context of fungal ingress. From the insertion of the palea to the base of the caryopsis proper, there are parenchymatous cells interspersed by blind vascular bundle endings. This tissue is called the "pedicel parenchyma" in the literature, but we prefer "floral axis parenchyma," in agreement with Arber (1), who viewed the stalk from the palea to the flower as a floral axis.

The anatomy of the caryopsis is well known (26,30–32) and will not be discussed here. However, two important features require mention. The pericarp consists of three layers: the epidemis or epicarp, the mesocarp, and the innermost endocarp (29,30). The last tissue lies adjacent to the testa (seed coat) and is aerenchymatous, its large airspaces arising from the differential growth of the pericarp tissues (30).

The other important feature of the maize kernel is the black layer (sometimes incorrectly referred to as the "hilar layer" [30]). This tissue develops in the chalaza as the grain approaches physiological maturity and is thought to prevent further apoplastic movement of assimilate (25). Johann (4) provided evidence that the black layer, whose chemical composition is unknown, was involved in resistance to fungal pathogens.

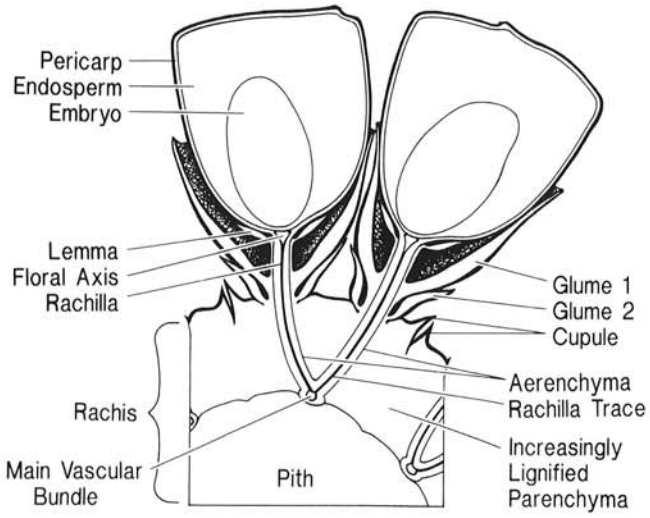

Fig. 1. Representation of a spikelet pair of the maize ear, seen in transverse section. The grains are in median longitudinal section. The parenchyma cells of the rachis are increasingly lignified as one proceeds outward from the pith (not lignified) to the fully lignified fibers directly beneath the cupule epidermis. The abortive florets and upper glumes and paleas of the fertile florets have been omitted for clarity.

MATERIALS AND METHODS

Maize (*Zea mays* L. DeKalb hybrid XL12) was grown in the Biotron at the University of Wisconsin, Madison, and inoculated with a mixture of isolates of *A. flavus* as previously described (22). Briefly, two sterile toothpicks were inserted on opposite sides of the midear region at 21 days after style (silk) emergence. They were pushed through the husks and developing grains as far as the lower rachilla or edge of the rachis. Each toothpick was withdrawn, dipped into a ten-isolate mixture of *A. flavus* conidia suspended in water (10^6 spores ml^{-1}, NRRL numbers as in 22), and replaced in the wounds. At 1, 3, 10, 14, and 28 days postinoculation (dpi), two ears were harvested for fungal isolations and fixation. The wounded spikelet and its two laterally adjacent, but unwounded, immediate neighbors were harvested. There were, therefore, four wounded and eight adjacent spikelets harvested at each time. The spikelets were excised, together with their underlying rachis segment, and halved longitudinally from pith to the grain crown. Those halves distal to the wounds were surface disinfested in 2% (w/v) NaOCl for 2 min, rinsed in sterile distilled water, and plated on malt-extract agar. The plates were incubated at 22 C in the dark and examined daily for hyphal growth under a stereomicroscope.

The other halves of the unwounded spikelets, the wounded spikelets, and their rachis segments were sliced into 5-mm cubes, and the pieces were grouped according to their position (grain crown; midgrain, lower grain, and proximal rachilla; distal rachilla, and rachis). The pieces were fixed in 5% (v/v) glutaraldehyde in 0.025 M sodium phosphate buffer, pH 6.9, at room temperature, under vacuum, for 3 hr. They were fixed a further 21 hr at 4 C and rinsed in cold buffer. Unless otherwise noted, the tissues were dehydrated in an homologous alcohol series in the cold and infiltrated with glycol methacrylate, (low acid, Polysciences, Inc., Warrington, PA) monomer mix (18) at 4 C for 3 mo. Once infiltration was adequate, the tissues were embedded at 68 C in the usual way (18). Some samples of each type of tissue block were postfixed in 2% (w/v) osmium tetroxide for 30 min at room temperature, dehydrated in an ethanol series, and embedded in an epoxy resin according to O'Brien and McCully (18). Trimmed blocks were sectioned at 1.5 μm on a Porter-Blum microtome (RMC, Inc., Tucson, AZ) and the sections affixed to glass slides for staining. Most blocks from each group were sectioned extensively, often completely. Survey sections were taken for examination every 50 to 300 μm, depending on whether they showed evidence of effects of the fungus in the

Figs. 2–7. 2, Hyphae of *Aspergillus flavus* permeate the rachilla of the wounded spikelet at 14 dpi. Hyphae are both intercellular and intracellular, but occasionally the fungus traverses the rachilla epidermis (arrow). AE, aerenchyma; Ep, epidermis; H, hyphae; and Hy, hypodermis. Scale = 20 μm. **3,** Infested bracts at 14 dpi. The bract cells collapse soon after fertilization, but the fungus grows on them to sporulate heavily. B, bracts in transverse section; Ep, epidermis; H, hyphae; S, spores (conidia); and SS, swollen spores (note remnants of the outer spore wall). Scale = 35 μm. **4,** Lignified fibers of the rachis cortex at 14 dpi. The cell walls are fully lignified and have neither intercellular spaces nor the fungus. The micrograph also is typical of fibers in material collected at 28 dpi. Note the cytoplasm pulled from the walls (arrows). F, fibers. Scale = 20 μm. **5,** Aerenchyma in the rachilla of the spikelet next to the wound at 14 dpi. Although no hyphae can be found here, the aerenchma cells have begun to collapse. AE, aerenchyma; CA, collapsed aerenchyma; and St, starch. Scale = 62.5 μm. **6,** Sparsely distributed hyphae in the lower rachilla of an unwounded spikelet at 28 dpi. The hyphae appear vacuolate and occur in the aerenchyma, outside the vascular tissue. The cells of the vascular bundle and aerenchyma are collapsed while xylem vessels contain a darkly staining material. AE, aerenchyma; BS, lignified bundle sheath; CA, collapsed aerenchyma; H, hyphae; P, phloem region; and X, xylem vessels. Scale = 30 μm. **7,** Narrow intercellular hyphae in the unlignified parenchyma of the rachis at 28 dpi. Hyphae are not seen to penetrate these cells. H, hyphae (also at arrowheads); I, intercellular space; and UL, lumina of unlignified parenchyma cells. Scale = 24 μm. All micrographs depict 1.5-μm thick sections of tissues fixed in glutaraldehyde and embedded in glycol methacrylate. Sections were doubly stained with the periodic acid-Schiff stain and toluidine blue O prior to examination.

region. Regions containing hyphae were sectioned closely to produce series of slides for detailed observation. Survey sections were stained with toluidine blue O, pH 4.5, for 5 min and rinsed. Sections for detailed observation were stained with the periodic acid-Schiff stain (19) and toluidine blue O, pH 4.5, before mounting in immersion oil. Sections were viewed and photographed in bright field optics on a Zeiss Photomicroscope I with plan-apochromat lenses and Kodak Plus-X Pan film, ASA 125.

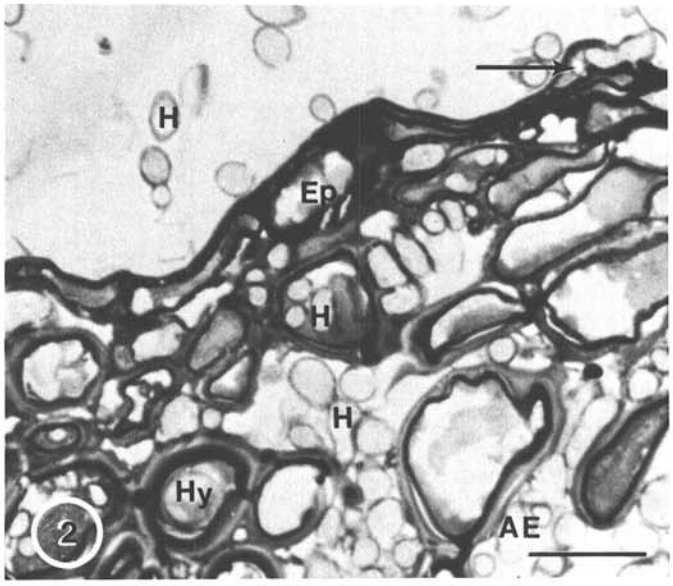

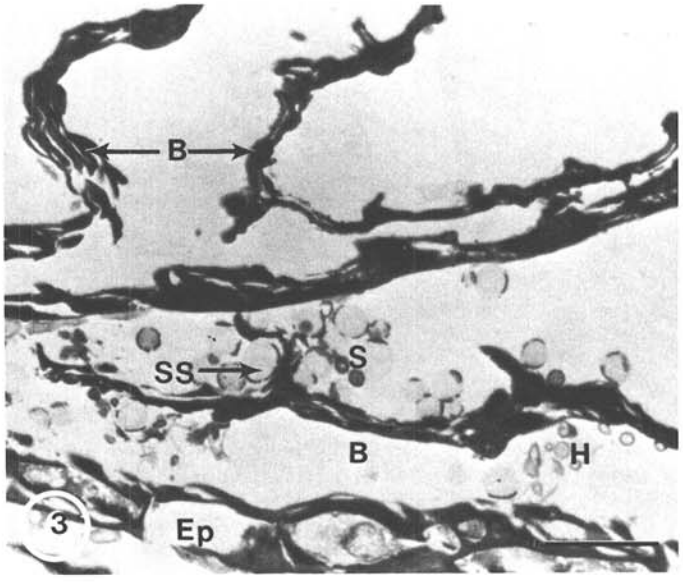

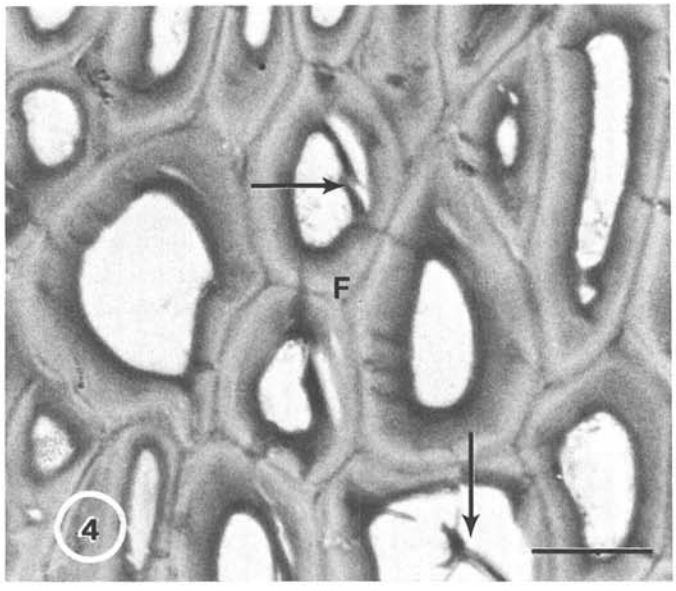

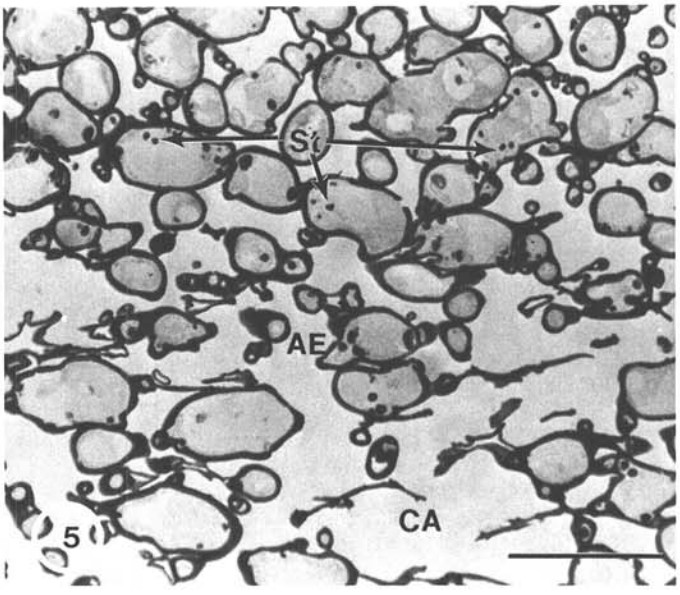

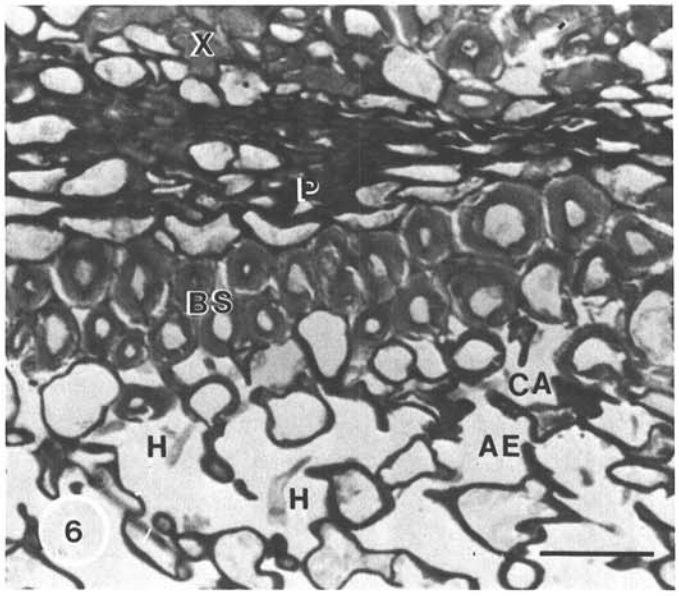

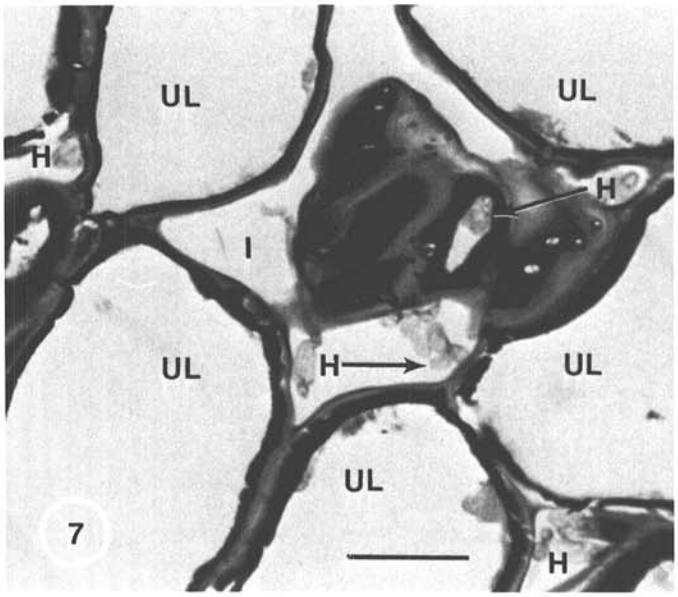

RESULTS

No fungal growth appeared on any spikelet half plated on agar at either 1 or 3 dpi. In contrast, 10 and 14 dpi spikelet halves showed fungal growth after incubation for 3 days. At first, hyphae grew only from the rachis segment and superficially on the grain crown. They were exceedingly sparse, often being only a few hyphal strands. Upon further incubation, these hyphae developed into typical colonies of *A. flavus*, complete with conidial heads. The conidia were typical of *A. flavus* in form, color, and size and were aggregated on globose vesicles. No contaminating microorganisms appeared on these plates even after incubation for 2 wk. The tissues sampled at 1 and 3 dpi were not examined microscopically because no fungal growth occurred on the plated material, and the results from 10 and 14 dpi sections (below) indicated that little fungus would be found, if any.

Microscopic examination of survey sections from material fixed at 10 and 14 dpi showed numerous hyphae in the rachilla of the wounded spikelet (Fig. 2). These hyphae were vacuolate but not collapsed and were both intercellular and intracellular. Occasionally, hyphae ruptured the epidermis, perhaps from inside the rachilla outward (Fig. 2). Macroscopically, the rachilla was discolored brown; and this was reflected in the deeply stained host-cell cytoplasms (Fig. 2). The bracts of the wounded spikelet also supported fungal growth on their surfaces (Fig. 3). These hyphae were vacuolate, and there were many conidia that appeared swollen. (Conidia were recognized primarily by their echinulate outer-wall architecture: swollen conidia had remnants of this wall [Fig. 3, see also Figs. 9 and 18].) The anticlinal walls of these infested bracts had collapsed (Fig. 3), but so had the anticlinal walls of the uninfested bracts (not shown). No cell wall dissolution was apparent. Hyphae were absent or very rare in the rachis tissues beneath the wound at 14 dpi. The lignified fibers (Fig. 4) found close to the rachis epidermis had few intercellular spaces and were not colonized by *A. flavus*. The normally parietal cell cytoplasm was disrupted (Fig. 4). This micrograph typifies the situation for lignified fibers in all subsequent tissues examined: even in infested 28 dpi rachis tissues, fibrous tissues were not colonized. Hyphae were absent from tissues of spikelets adjacent to the wound at 10 and 14 dpi, even though these tissues were surveyed extensively, with equal emphasis on the pericarp, embryo, rachilla, and underlying rachis. This is not to say that the tissues were undisturbed. The rachilla aerenchyma cells had begun to collapse (Fig. 5), even though other nearby cells were apparently healthy and contained starch. We should note here that we planned to examine sections of wounded, but uninoculated, control tissues. Unfortunately, all uninoculated wounds became infested with *Aspergillus niger* Tiegh. and, hence, were not harvested. The collapse of aerenchyma cells mentioned here and elsewhere as a concomitant of disease caused by *A. flavus* probably is not an artifact, since similar tissues wounded and inoculated with *Gibberella zeae* (Schwein.) Petch show little evidence of aerenchyma cell collapse even when heavily infested (M. G. Smart, *unpublished*). However, the phenomenon requires confirmation.

Tissues plated on malt extract agar after harvest at 28 dpi were quickly overgrown with *A. flavus*. The pathogen also showed the greatest extent of development in tissues fixed at 28 dpi. In general, the hyphae were present, to a greater or lesser degree, in all tissues from the rachilla of the wounded spikelet to the rachillae, pericarps, and embryos of neighboring spikelets, including the intervening rachis. The grains of wounded spikelets were mere remnants of pericarp tissues at 28 dpi and usually were without any structure.

In the lower part of the wounded rachilla, distal to the wounded grain, hyphae were intercellular and appeared highly vacuolate (Fig. 6). The fungus became less common further from the wounded grain, and the individual hyphae were narrower in diameter. Again, aerenchyma cells were wholly or partly collapsed, as were cells of the vascular bundle (Fig. 6). In particular, the cells of the phloem region were grossly distorted, and the xylem vessels contained a darkly stained material which was periodic acid-Schiff stain and toluidine blue O positive. No hyphae were seen inside the bundle sheath fibers in these vascular bundles. Collapsed phloem, xylem vessels with stainable contents, and an absence of any fungus inside the bundle sheath fibers were consistent features of all vascular bundles up to and including those of the rachilla of the neighboring spikelets.

Both unlignified and lignified parenchyma tissues of the rachis had hyphae in their intercellular spaces (Figs. 7,8). The hyphae were narrow in cross section and without stainable contents. Although the presence of the fungus was often quite rare, hyphae could be found in the rachis parenchyma intercellular spaces beneath the wounded spikelet and beneath the neighboring spikelets. The host cells often had darkly stained cytoplasm, which was usually in its normal parietal position (Figs. 7,8). The two exceptions where no hyphae were found were the fibers of the outer rachis (mentioned above) and the pith.

The outstanding feature of Figure 8, of course, is the presence of curious circular objects inside the cell. Such cells were relatively common in the lignified parenchyma. This particular cell (in Fig. 8) was sectioned serially at 1.0 μm and then reconstructed with a computer software program for three-dimensional imaging (Jandel Scientific, CA). This cell was intact, meaning that, other than a single fungal penetration site, the walls were unbroken. The circular objects in the cell were spherical when reconstructed; and the small, darkly stained ones were within the size range for *A. flavus* conidia. Neither hyphae nor typical *A. flavus* conidiophores were seen in this or any other cell of the rachis.

A feature of the mode of insertion of all maize floral bracts (glumes, paleas, and lemmas) on the rachilla is illustrated in Figure 9. This bract, a glume, typifies the arrangement. The section passed through the adaxial region of the insertion site. Most of the cells are large, thin-walled, and highly vacuolate. Even the hypodermal fibers have large airspaces between them. Thus, there was airspace continuity from the aerenchyma to the border of the insertion site. The crushed epidermal cells were sometimes torn at the border, thus completing continuity between the exterior environment (i.e., beneath the husks) and the aerenchyma in the center of the rachilla. Hyphae could be seen throughout these airspaces (Fig. 10) and in the aerenchyma (Fig. 11). Note the extensive cell collapse of the aerenchyma (Figs. 9,11). As before, hyphae were rarely found, were vacuolate, and were relatively

Figs. 8–13. 8, Intercellular hyphae and intracellular spores in the lignified parenchyma of the rachis at 28 dpi. Normal-sized and swollen conidia occur in the cell lumen. The clear areas within the cell are actually grossly swollen conidia, which have lost all contrast, but remnants of their original walls can be seen (arrows). H, intercellular hyphae; L, lignified parenchyma; S, conidia; and SS, swollen conidia. Scale = 24 μm. **9,** Junction zone of a glume and the rachilla in an unwounded spikelet at 28 dpi. The normally continuous hypodermis becomes disrupted at the junction zone (double arrows), leaving large, thin-walled cells to fill the gaps. Note the extensive cell collapse in the aerenchyma. B, bract; CA, collapsed aerenchyma; Hy, hypodermis; and J, junction zone. Scale = 125 μm. **10,** High magnification view of a junction zone with hyphae throughout. The fungus (at arrowheads) permeates the zone. AE, aerenchyma; H, hyphae; and J, junction zone. Stained with periodic acid-Schiff stain and toluidine blue O. Glutaraldehyde/osmium fixation embedded in epoxy resin. Scale = 32 μm. **11,** Rare hyphae in the rachilla aerenchyma of an unwounded spikelet at 28 dpi. The hyphae are vacuolate amid general collapse of the aerenchyma cells. CA, collapsed aerenchyma; H, hypha; and St, starch. Scale = 20 μm. **12,** Hyphae in the floral axis ("pedicel parenchyma") of an unwounded spikelet at 28 dpi. Many hyphae are collapsed or otherwise vacuolate while floral axis cells have broken down, allowing intracellular growth. Fp, floral axis parenchyma; and H, hyphae. Scale = 20 μm. **13,** Hyphae in the endosperm cavity do not cross the black layer of an unwounded spikelet at 28 dpi. BL, obliquely cut black layer cells (without fungus); EN, endosperm cavity; F, floral axis; and H, densely cytoplasmic hyphae. Scale = 20 μm. All micrographs except Figure 10 depict 1.5-μm thick sections of tissues fixed in glutaraldehyde and embedded in glycol methacrylate. Sections were doubly stained with the periodic acid-Schiff stain and toluidine blue O prior to examination.

narrow in diameter.

Hyphae became more common in the upper rachilla (proximal to the unwounded grain) and permeated the parenchyma of the floral axis (the so-called "pedicel parenchyma," Fig. 12). In addition to being vacuolate, many hyphae appeared to be collapsed. They were extracellular except where host cells were broken (Fig. 12). Profiles similar to these were seen in the schizogenous space which forms in the black layer during grain maturation. The black layer itself was not traversed by hyphae, despite their abundance in the endosperm (Fig. 13), where they were densely cytoplasmic and not collapsed (Fig. 13).

In the pericarp, the fungus was found in the endocarp (Figs.

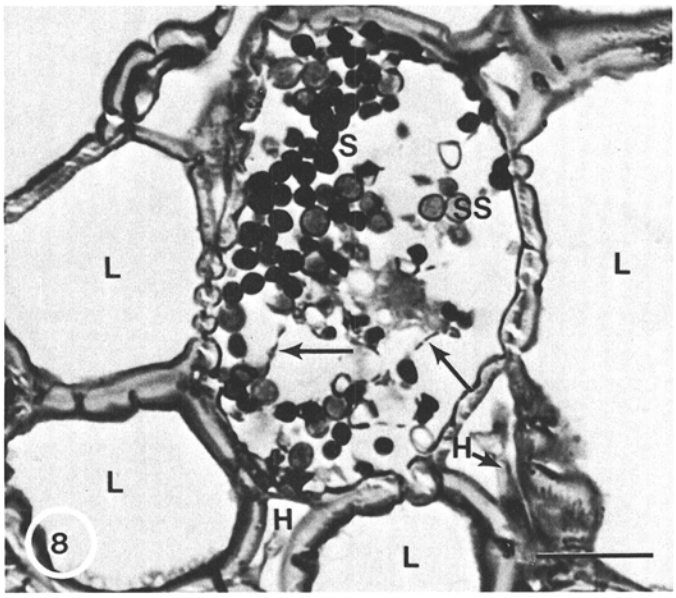

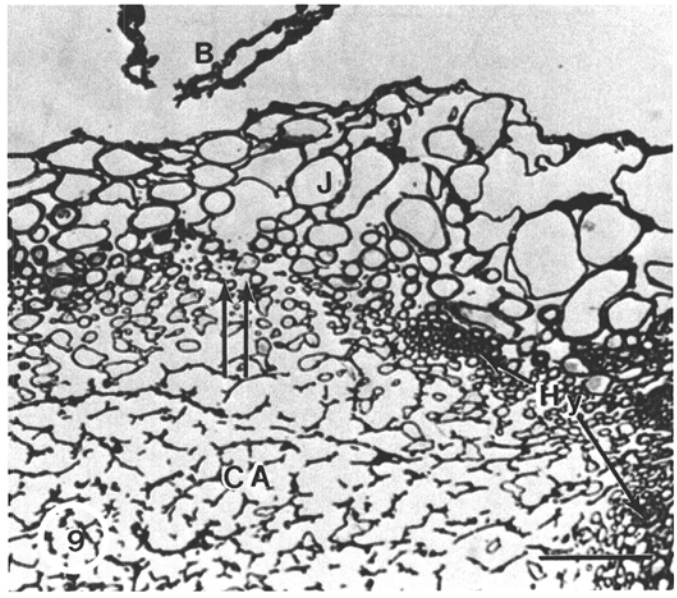

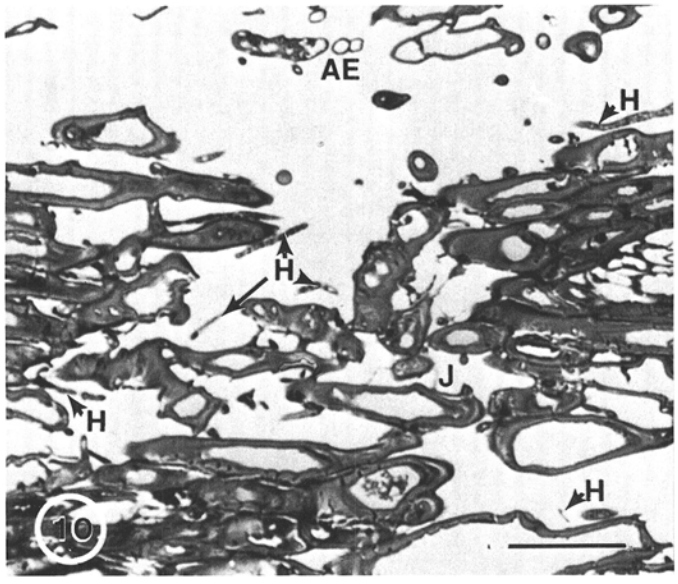

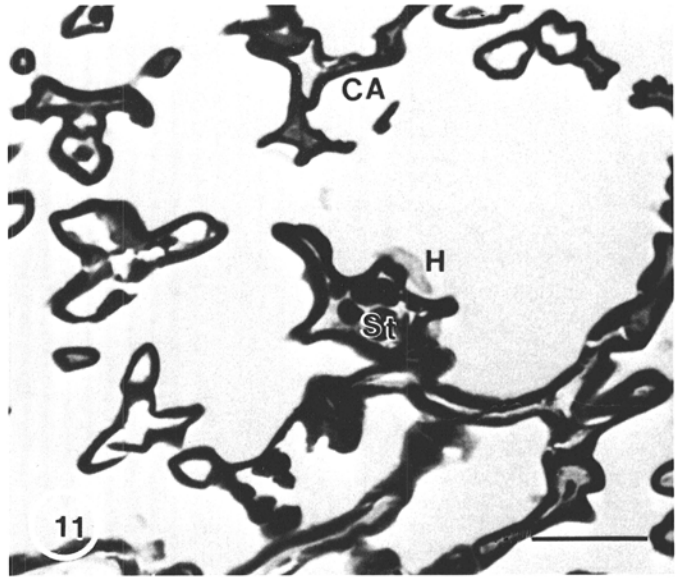

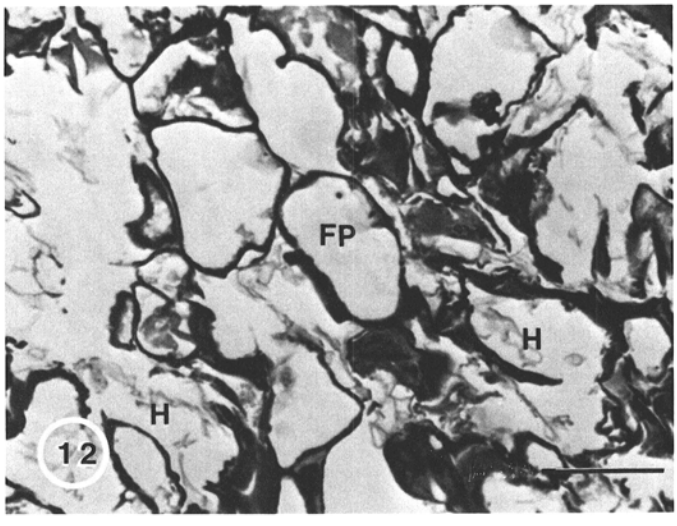

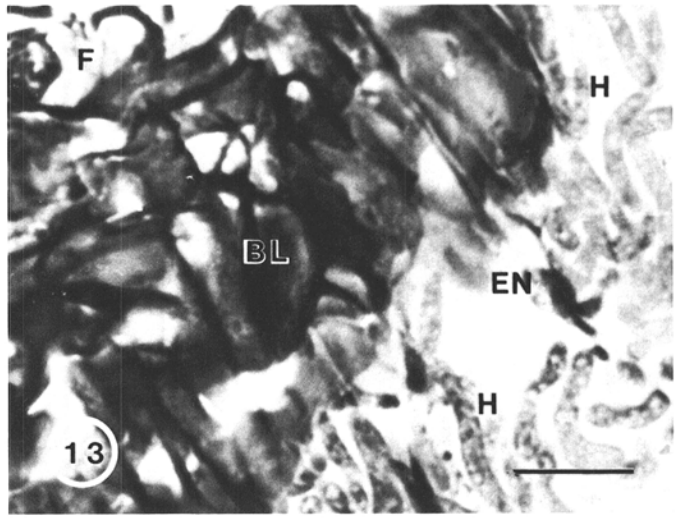

14,15) and in the mesocarp (Fig. 14), but not in the epicarp. Hyphae were not common anywhere in the pericarp as a whole, although locally high concentrations were seen (Fig. 14). In general, the upper portion of the grain was without fungus, as was most of the dorsal face of the grain. Only over the embryo and in the center of the dorsal face were hyphae seen. Sporulation was possible in these regions of the endocarp (Fig. 15). The cell walls of the mesocarp were deep blue to aqua when stained with toluidine blue O. These mesocarp cells showed the only instance of localized wall dissolution outside the testa. The associated hyphae were small and vacuolate, as we had come to expect outside the testa.

The embryos of unwounded grains adjacent to the inoculation site were invaded (Figs. 16,17,19). Hyphae were common in all embryonic tissues but particularly the scutellum (Figs. 16,17). The fungus was densely cytoplasmic with broad hyphae ramifying intercellularly and intracellularly, penetrating or even apparently dissolving walls in their paths (Figs. 16,17). The integrity of scutellum cell cytoplasm was lost ahead of the hyphae (Fig. 18), although starch grains appeared unaffected.

The fungus invaded the aleurone cells (Fig. 19). At a distance of 1–2 mm from the embryo, hyphae were found first in the crushed nucellar epidermis, between the seed coat cuticle and the aleurone layer (not shown). Entry into the seed was apparently effected by the fungus simply growing through breaks in the seed coat cuticle (Fig. 19). Sporulation occurred in any airspace (between embryo and the aleurone, around the coleoptile and coleorhiza, and in spaces of the endosperm). The fungus was not common in the endosperm except close to the scutellum.

DISCUSSION

Our results show that *A. flavus* can grow from a wound-inoculation site to infest unwounded spikelets in two ways: It can grow superficially over rachis and spikelet surfaces to invade at the junction of the bracts with their rachillas. Or, the pathogen can grow through the internal airspace continuum of the rachis and spikelets. We have never observed direct penetration of the grain through the epicarp, the epidermis of the pericarp; all endocarp infestation arises fom hyphae entering the grain from the upper rachilla. The first of these alternatives support the view of Marsh and Payne (15,16). Based upon their own findings for *A. flavus* and those in the literature for other ear-rotting fungi (4,10,14), they proposed that style-inoculated ears must be invaded somewhere along the rachilla. But, since they examined grains shelled from the ear prior to fixation, they missed the largest area of penetrable tissue: the adaxial zone of the rachilla at the glume insertion site. (The glumes, together, completely surround the rahilla at their insertion. It is no accident, then, that the grains disarticulate at this site because it would be the weakest part of the rachilla. We assume that, during development, this region replaces stomata in function, allowing gaseous exchange for the embryo.) Penetration of this region has not previously been seen for any disease of maize ears, although Johann (4) apparently suspected it. The other bracts (the two paleae and two lemmas) also have this peculiar anatomical feature. Since their insertion sites are smaller, they probably are less frequently areas of penetration. Certainly we did not observe fungal ingress into the rachilla at these smaller bracts. Strictly speaking, we cannot claim to have seen fungal ingress at the glume junction zones. Since we only found hyphal growth at 28 dpi, and since the pathogen can spread in two ways, the hyphae depicted in Figure 10 could have been egressing from the aerenchyma. Nevertheless, we are confident that this zone represents a major ingress site for this, and other, pathogens.

The literature scarcely mentions the spread of any ear pathogen through the rachis, that is, the second of the two alternative means used by *A. flavus*. We are aware of no micrographs depicting it. Manns and Adams (14) considered growth through the rachis a possibility for various fungi, including *D. zeae* and *Fusarium moniliforme* Sheldon, but were not definite on the point. *F. moniliforme*, in particular, is said to be "systemic," but very little histology supports this view (11). We found growth through the rachis, at least for *A. flavus*, since there are no physical barriers to be overcome. The fungus simply ramifies throughout the airspaces, if sparsely, but rarely actually invades rachis cells. When it does invade rachis cells, the fungus sporulates, producing many conidia. We saw no conidiophores or hyphae in these cells, but these structures may have been obliterated by the development of conidia and not visible given the resolution of the light microscope. The survival value of this phenomenon in cobs overwintering on the ground may be signficant.

Since the fungus was found in the rachis airspaces between the wound and adjacent spikelets only at 28 dpi, we cannot judge the relative importance of this mode of hyphal spread versus that of over the pericarp to the bract junctions. Further study of events between 14 and 28 dpi should clarify this situation. Our results imply that growth occurred late in the development of the maize ears (that is, after 14 dpi). This agrees with previously published data (5,20). We were surprised that all hyphae outside the seed coat cuticle were vacuolate (and even partly collapsed in the floral axis). There is a possibility that this was, in part, an artifact of glycol methacrylate embedding, since osmium-fixed fungal tissues sometimes appeared more densely cytoplasmic (see Fig. 10). However, because fungal tissues internal to the seed coat cuticle were always densely cytoplasmic, even in glycol methacrylate embedded material (Figs. 16,17), we believe there is some difference in the two environments (on either side of the seed coat cuticle), which resulted in the different images.

Whatever the reason for the differences in hyphal morpology, it is clear that the pathogen destroys host cells ahead of itself (Figs. 4,5,18). The collapse of aerenchyma cells and vascular bundles is an unusual host response. The phenomenon was real enough because we observed it in hand sections of unfixed material. As we have observed above, the cell collapse in the aerenchyma was seen rarely in similar tissues infested with *G. zeae* and, thus, would seem to be specific to the *Aspergillus*-maize interaction. However, definitive assignment of aerenchyma cell collapse as a host response to *A. flavus* must await studies in which hyphal development is more closely monitored between

Figs. 14–19. 14, Hyphae in the pericarp of an unwounded grain at 28 dpi. Vacuolate hyphae in the endocarp and mesocarp are not common overall, but in localized areas they dissolve cell walls of the latter. The hyphae do not penetrate the seed coat cuticle (hyaline structure on the nucellus) here. AL, aleurone layer; E, endocarp; H, hyphae; M, mesocarp; and N, nucellus. Scale = 32 μm. **15,** Conidial heads with phialides in the endocarp at 28 dpi. Conidiophores were locally common in the endocarp over the embryo; some of the phialides and swollen spores can be seen here. (Note remnants of the original spore wall on the conidium at SS.) C, conidial head with phialides; S, conidia (normal spores); and SS, swollen conidia. Scale = 35 μm. **16 and 17,** Two views of the scutellum in an unwounded grain infested with *A. flavus* at 28 dpi. The hyphae are broad, densely cytoplasmic, intercellular, and intracellular. The fungus can penetrate cells directly (arrow, Fig. 15). The normal reserves of an embryo are disorganized, except for starch, and some parts of the cell walls are even dissolved (double arrows, Fig. 16). H, hyphae; Sp, scutellum parenchyma; St, starch; and V, provascular tissue. Scales = 30 μm (Fig. 16) and 24 μm (Fig. 17). **18,** The scutellum parenchyma reserves and cytoplasm are disturbed ahead of the fungus at 28 dpi. No protein bodies, lipid droplets, or phytin are visible while starch is unaffected. The cell walls are intact (arrows at pitfields) in this region. N, nucleus; Sp, scutellum parenchyma; and St, starch. Scale = 30μm. **19,** Inward, random breaks in the seed coat cuticle (double arrows) probably allow fungal ingress. The hyphae ramify through the crushed nucellar epidermis, the aleurone, and the embryo. AL, aleurone layer; E, endocarp; H, hyphae; and Sc, scutellum. Phase-contrast optics. Scale = 30 μm. All micrographs depict 1.5 μm thick sections of tissues fixed in glutaraldehyde and embedded in glycol methacrylate. Sections were doubly stained with the periodic acid-Schiff stain and toluidine blue O prior to examination.

14 and 28 dpi. The cause could possibly be aflatoxin, except that we cannot find proof of aflatoxin transport (22), and the phytotoxic effects of aflatoxin are not well known. Whatever the cause, the cell death implied by this result might restrict possiblities for chemical defense responses by the host. However, we were unable to determine the relative timing of host cell collapse, tannin formation, and hyphe growth, and, therefore, cannot address this question.

Of course, it is the penetration of hyphae into the seed, and their subsequent growth in the embryo, which is of paramount importance economically. The fungus apparently gains access to the seed from the endocarp by growing through breaks in the testa immediately over the embryo. Again, we say "apparently" because we have only one time point where the phenomenon was observed. But invaded seeds always had a broken testa (here, more or less synonymous with the seed coat cuticle), and the

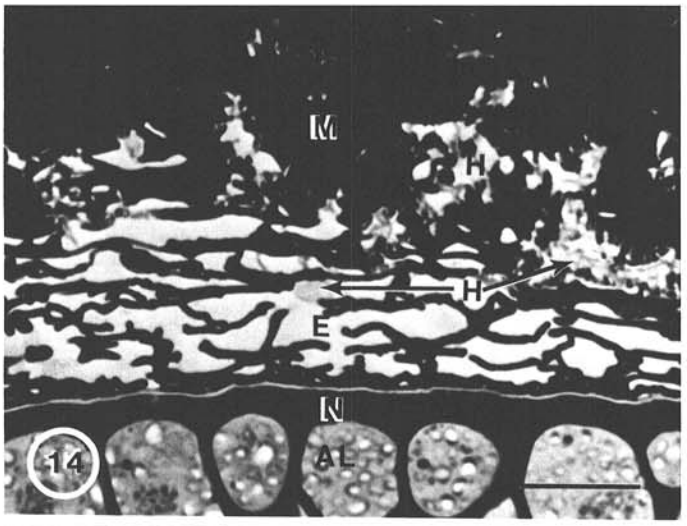

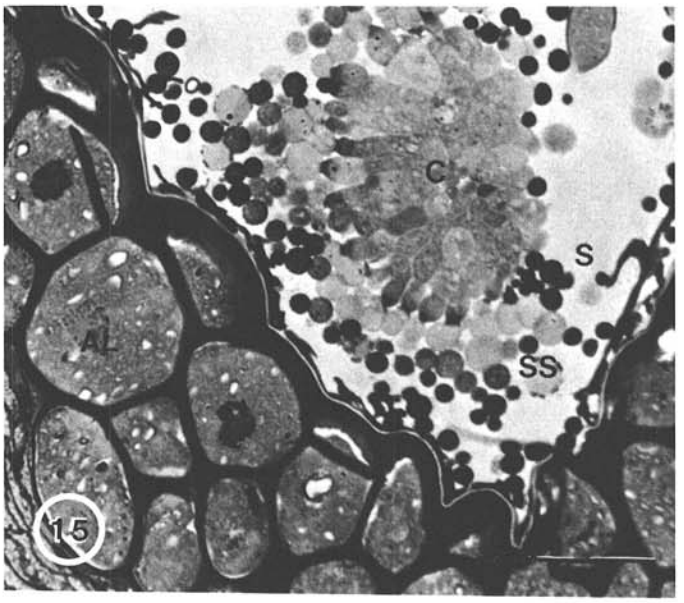

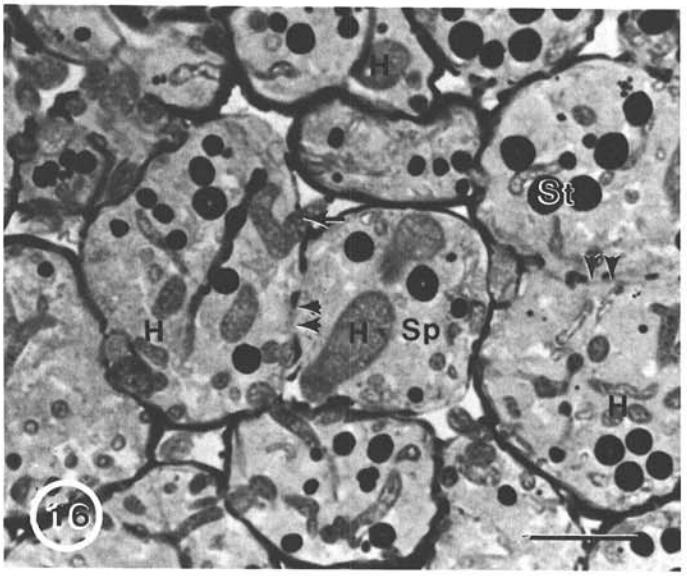

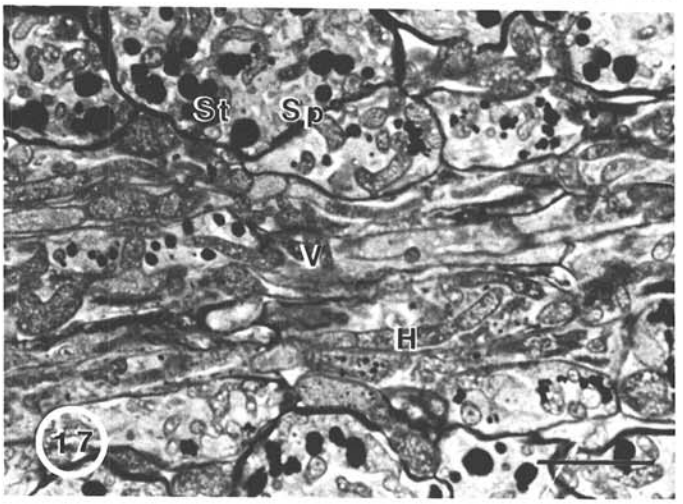

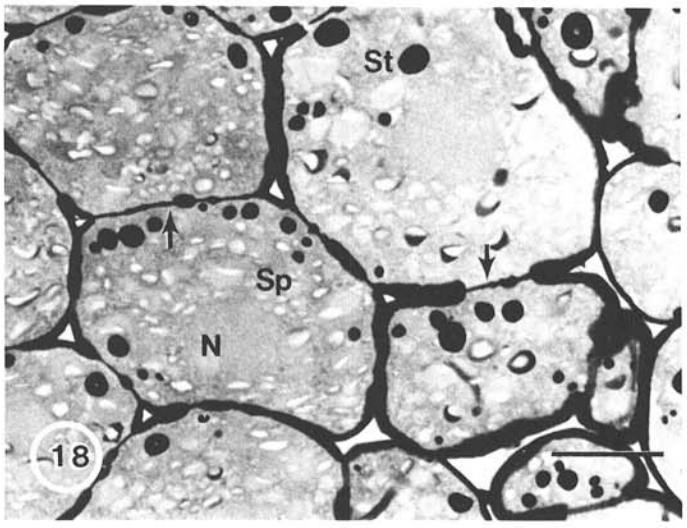

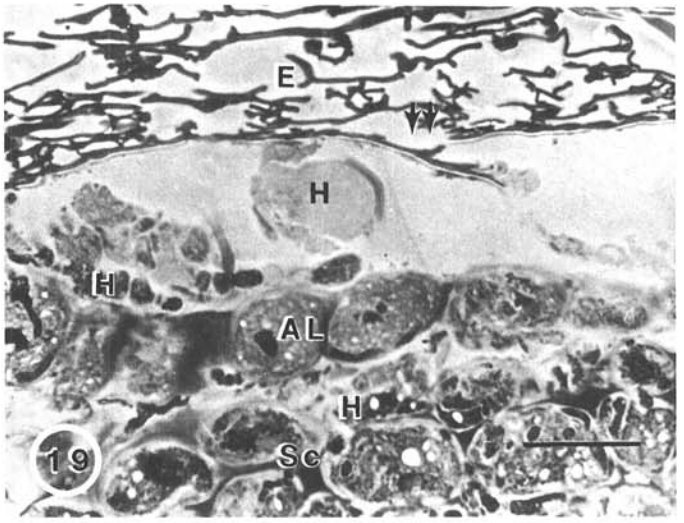

breaks were inward, seemingly ruling out the possibility that the fungus produced the breaks by exiting from the embro into the pericarp. Our previous data (22) showed that *A. flavus* invaded maize seeds randomly. We assume that the breaks are random, too. What factors cause these breaks we cannot be sure, except that the appearance of darkly staining material in the xylem vessels ahead of the fungus may imply altered water relations in the ear. This could lead to uneven drying down in the caryopses (embryo versus endosperm), resulting in testa disruption. Adverse weather conditions, particularly drought, are known to exacerbate disease due to *A. flavus* (2). The presence of vivipary genes (17) in a hybrid is obviously also potentially deleterious.

In earlier Biotron experiments where DeKalb XL12 was wound inoculated with *A. flavus* (temperature 30/20 C for 14/10 hr day/night cycle), the fungus grew from 75–98% of surface-disinfested, intact grains in individual ears (28,29). Samples of intact grains that were separated from the wound site by two or more grains showed substantial levels of aflatoxin contamination for some of the ears. We initially designed and carried out this present study at these lower temperatures using a single *A. flavus* isolate. However, after sectioning many grains and analyzing many mosaics for aflatoxin, both of which failed to show any evidence of the fungus except in the wounded rachilla, we abandoned this approach in favor of the current multi-isolate, high-temperature one. Presumably, in the earlier work of Wicklow and coworkers (28,29), the fungus did spread from the inoculation site, but often may have been reisolated from the floral axes of the unwounded grains. In general terms, we suggest that stress injury to maturing grains grown at high temperatures leads to cracks in the testa and allows internal colonization of the grains, chiefly the embryonic tissues and the aleurone layer. Such stresses may occur more often in the southern United States, where aflatoxin contamination is more prevalent.

The literature is unclear about the role of the black layer in host defense. Johann (4) felt that resistance to various ear pathogens (but she did not consider *A. flavus*) was correlated with rapid maturation of the "closing layer" forming the black layer. She depicts hyphae of *D. zeae* throughout the region in developing grain. For *A. flavus*, the black layer was well formed by 14 dpi, before hyphal growth began from the wound. We never saw hyphal penetration of the seed through this region. Indeed, *A. flavus* rarely penetrated any cell type and never penetrated cuticularized cell walls. The chemical composition of the black layer is unknown, but it probably is lignified, suberized, or both. In our experience, it resists fungal penetration, but the late development of the pathogen makes an active role of the black layer in resistance to *A. flavus* unlikely.

LITERATURE CITED

1. Arber, A. 1934. The Gramineae. Cambridge University Press. Cambridge, England.
2. Diener, U. L., Cole, R. J., Sanders, T. H., Payne, G. A., Lee, L. S., and Klich, M. A. 1987. Epidemiology of aflatoxin formation by *Aspergillus flavus*. Annu. Rev. Phytopathol. 25:249-270.
3. Esau, K. 1965. Plant Anatomy. 2nd ed. John Wiley and Sons, Inc., New York. 767 pp.
4. Johann, H. 1935. Histology of the caryposis of yellow dent corn, with reference to resistance and susceptibility to kernel rot. J. Agric. Res. 51:855-853.
5. Jones, R. K., Duncan H. E., and Hamilton, P. B. 1981. Planting date, harvest date, and irrigation effects on infection and aflatoxin production by *Aspergillus flavus* in field corn. Phytopathology 71:810-816.
6. King, S. B., and Scott, G. E. 1982. Field inoculation techniques to evaluate maize for reaction to kernel infection by *Aspergillus flavus*. Phytopathology 72:782-785.
7. Kisselbach, T. A. 1949. The structure and reproduction of corn. Neb. Agric. Exp. Stn. Res. Bull. 161. 96 pp.
8. Klich, M. A., and Chmielewski, M. A. 1985. Nectaries as entry sites for *Aspergillus flavus* in developing cotton bolls. Appl. Environ. Microbiol. 50:602-604.
9. Klich, M. A., Thomas, S. H., and Mellon, J. E. 1984. Field studies on the mode of entry of *Aspergillus flavus* into cotton seeds. Mycologia 76:665-669.
10. Koehler, B. 1942. Natural mode of entrance of fungi into corn ears and some symptoms that indicate infection. J. Agric. Res. 64:421-442.
11. Lawrence, E. B., Nelson, P. E., and Ayers, J. E. 1981. Histopathology of sweet corn seed and plants infected with *Fusarium moniliforme* and *F. oxysporum*. Phytopathology 71:379-386.
12. Laubengayer, R. A. 1949. The vascular anatomy of the eight-rowed ear and tassel of golden bantam sweet corn. Am. J. Bot. 36:236-244.
13. Lee, L. S., Lillehoj, E. B., and Kwolek, W. F. 1980. Aflatoxin distribution in individual corn kernels from intact ears. Cereal Chem. 57:340-343.
14. Manns, T. F., and Adams, J. F. 1923. Parasitic fungi internal of seed corn. J. Agric. Res. 23:495-524.
15. Marsh, S. F., and Payne, G. A. 1984. Scanning EM studies on the colonization of dent corn by *Aspergillus flavus*. Phytopathology 74:557-561.
16. Marsh, S. F., and Payne, G. A. 1984. Preharvest infection of corn silks and kernels by *Aspergillus flavus*. Phytopathology 74:1284-1289.
17. Neuffer, M. G., Jones, L., and Zuber, M. S. 1968. The Mutants of Maize. Crop Science Society of America, Madison, WI.
18. O'Brien, T. P., and McCully, M. E. 1981. The Study of Plant Structure, Principles and Selected Methods. Termacarphi Pty. Ltd., Wantirna, Australia.
19. Payne G. A., Hagler, W. M., and Adkins, C. R. 1988. Aflatoxin accumulation in inoculated ears of field-grown maize. Plant Dis. 72:422-424.
20. Payne, G. A., Thompson, D. L., Lillehoj, E. B., Zuber, M. S., and Adkins, C. R. 1988. Effect of temperature on the preharvest infection of maize kernels by *Aspergillus flavus*. Phytopathology 78:1376-1380.
21. Reeves, R. G. 1950. Morphology of the ear and tassel of maize. Am. J. Bot. 37:697-704.
22. Smart, M. G., Shotwell, O. L., and Caldwell, R. W. 1990. Pathogenesis in Aspergillus ear rot of maize: Aflatoxin B_1 levels in grains around wound-inoculation sites. Phytopathology 80:1283-1286.
23. Taubenhaus, J. J. 1920. A study of the black and the yellow molds of ear corn. Tex. Agric. Exp. Stn. Bull. 270. 88 pp.
24. Thompson, D. L., Payne, G. A., Lillehoj, E. B., and Zuber, M. S. 1983. Early appearance of aflatoxin in developing corn kernels after inoculation with *Aspergillus flavus*. Plant Dis. 67:1321-1322.
25. Thorne, J. N. 1985. Phloem unloading of C and N assimilates in developing seeds. Annu. Rev. Plant Physiol. 36:317-343.
26. van Lammeren, A. A. M. 1986. Developmental morphology and cytology of the young maize embryo (*Zea mays* L.). Acta Bot. Neerl. 35:169-188.
27. Weatherwax, P. 1916. Morphology of the flowers of *Zea mays*. Bull. Torrey Bot. Club 43:127-144.
28. Wicklow, D. T., Horn, B. W., and Shotwell, O. L. 1987. Aflatoxin formation in preharvest maize ears. Mycologia 79:679-682.
29. Wicklow, D. T., Horn, B. W., Shotwell, O. L., Hesseltine, C. W., and Caldwell, R. W. 1988. Fungal interference with *Aspergillus flavus* infection and aflatoxin contamination in maize grown in a controlled environment. Phytopathology 78:68-74.
30. Wolf, M. J., Buzan, C. L., MacMasters, M. M., and Rist, C. E. 1952. Structure of the mature corn kernel. I. Gross anatomy and structural relationships. Cereal Chem. 29:321-333.
31. Wolf, M. J., Buzan, C. L., MacMasters, M. M., and Rist, C. E. 1952. Structure of the mature corn kernel. II. Microscopic structure of the pericarp, seed coat and hilar layer of dent corn. Cereal Chem. 29:334-348.
32. Wolf, M. J., Buzan, C. L., MacMasters, M. M., and Rist, C. E. 1952. Structure of the mature corn kernel. III. Microscopic structure of the endosperm of dent corn. Cereal Chem. 29:349-361.
33. Wolf, M. J., Buzan, C. L., MacMasters, M. M., and Rist, C. E. 1952. Structure of the mature corn kernel. IV. Microscopic structure of the embryo of dent corn. Cerel Chem. 29:362-381.